Proceedings of the 1st International Symposium on Steel Science (IS^3-2007) ,
The Iron and Steel Institute of Japan, 2007

Stress State and Strain Rate Dependence of the Strain-induced Martensitic Transformation in a Metastable Austenitic Stainless Steel

Peter Hedström[1*], Lars-Erik Lindgren[2] and Magnus Odén[3]

[1]Division of Engineering Materials, Luleå University of Technology, 971 87 Luleå, Sweden
[2]Division of Material Mechanics, Luleå University of Technology, 971 87 Luleå, Sweden
[3]Nanostructured Materials, Dept Physics, Linköping University, 581 83 Linköping, Sweden

Abstract: The strain-induced martensitic transformation in a metastable austenitic stainless steel is investigated by high-energy x-ray diffraction and material modeling. Two different deformation modes are used (cold rolling and uniaxial tensile loading) and the effect on the strain-induced martensitic transformation behavior is investigated. Moreover, three different strain rates during the uniaxial tensile loading are evaluated.

The results show a sigmoidal transformation behavior of the strain-induced martensite in respect to true strain, for tensile loading. The effect of different strain rates is also clearly seen and it alters both the amount of transformed martensite and the transformation behavior. The martensite transformation is drastically decreased already at moderate strain rates such as 10^{-2} s^{-1}, due to adiabatic heating of the sample.

The material model used gives an accurate prediction of the strain-induced martensitic transformation behavior during tensile loading. This is valuable for further implementation of the current material model in industrial forming simulations of real components.

1. INTRODUCTION

The metastable austenitic stainless steels are susceptible to a deformation-induced martensitic phase transformation improving the strain hardening and the time to neck formation [1, 2]. This martensitic transformation is strain-induced at ambient temperatures [3] and the martensite embryos form at new nucleation sites generated by the deformation, e.g. shear-band intersections. Since the strain-induced martensitic transformation is deformation dependant it is affected by the deformation characteristics, such as deformation mode and strain rate. There are numerous studies of these deformation characteristics and previous investigations have for instance shown that more ά-martensite is generated for a biaxial stress state, compared to uniaxial loading. Olson and Cohen [3] predicted that the strain rate would impact the strain-induced martensite transformation in two ways, where a high strain rate might be beneficial for generating more nucleation sites for the martensite, but the martensite will also induce adiabatic heating of the samples which is known to decrease the amount of martensite transformation [4].

In order to perform forming simulations of the metastable austenitic stainless steels it is vital to predict the strain-induced martensite accurately. The mechanical properties can then be estimated based on the phase composition and the individual phases' properties. Here we report on initial results from high-energy x-ray diffraction experiments and material modeling investigating the stress state and strain rate dependence of the strain-induced martensitic transformation in a metastable austenitic stainless steel is presented. This constitutes necessary improvements of the constitutive equations in industrial forming simulations of real components.

2. MATERIALS AND METHODS

Metastable austenitic stainless steel AISI 301 supplied by Outokumpu Stainless was investigated. The steel sheets were delivered in annealed condition with 1 mm thickness and in cold rolled condition suffering reductions up to 61%. For chemical composition, see Table 1. The microstructure of an annealed steel sheet is depicted in Fig. 1a, which demonstrates a fully austenitic structure and a grain size of about 30 μm. In Fig. 1b a micrograph of a 61% cold rolled sample is displayed. This microstructure consists of austenite, ά-martensite and ε-martensite.

Table 1: Chemical composition in wt%

Fe	Cr	Ni	Mn	Si	Mo	Cu	Co	C	N	Nb
Bal.	17.55	7.67	1.23	0.55	0.31	0.25	0.1	0.095	0.022	0.008

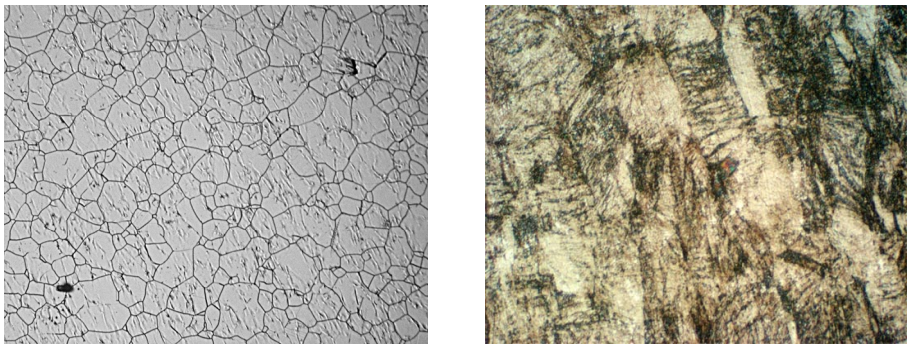

Fig. 1: a) Optical micrograph of AISI 301 in annealed condition. The sample was mechanically polished, electro-polished and subsequently grain boundary etched b) Optical micrograph of AISI 301 suffering 61% cold rolling reduction. The sample was mechanically polished, electro-polished and martensite etched

2.1 Experimental

High-energy x-ray diffraction experiments were conducted at the 1-ID beamline at the Advanced Photon Source (APS). The used x-ray wavelength was 0.2001Å and the beam size was 1mmx1mm. The experiments were performed in transmission geometry, enabling bulk measurements (Fig. 2). For fast sampling of diffraction patterns an area detector placed 740 mm from the specimen was used. *In situ* experiments during tensile loading were performed by mounting the samples in a load rig and the strain was measured using a miniature extensometer and for high strains the position of gage heads at the load rig was instead used. CeO_2 powder was attached to all samples for calibration of the setup geometry. The high-energy x-ray diffraction experiments were complemented with lab-scale diffractometry using CuK_α (1.5418Å). Two dimensional diffraction patterns from the GE-detector were integrated over 360° in azimuth to one dimensional diffraction patterns, see Fig. 3. The peak positions and integrated intensities were subsequently determined for all diffraction patterns by least squares fitting of a pseudo-Voigt function.

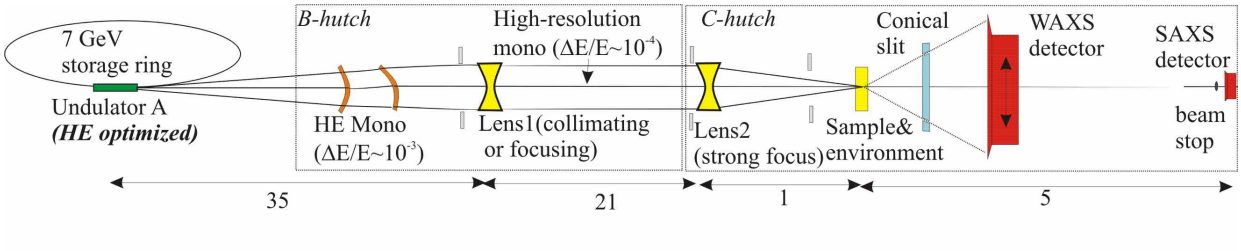

Fig. 2: High-energy x-ray diffraction setup at the 1-ID beamline at the Advanced Photon Source. A small angle x-ray scattering detector for SAXS experiments and a conical slit for spatial resolution along the beam can also be used in this setup. Approximate distances are given in unit meters.

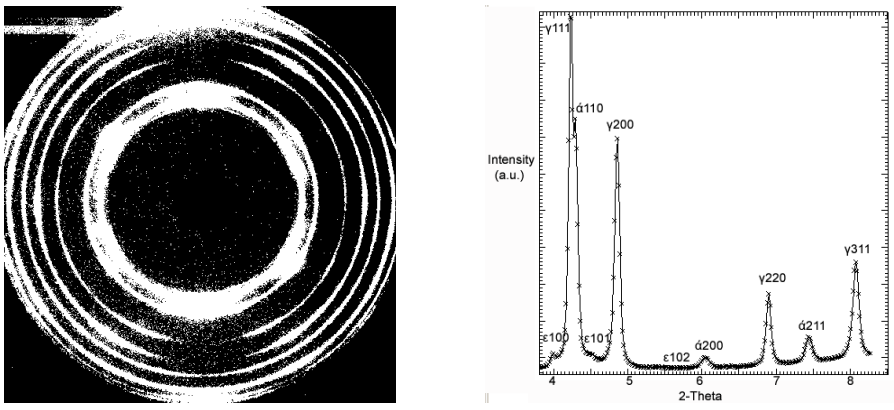

Fig. 3: a) Two dimensional diffraction pattern of AISI 301 b) One dimensional diffraction pattern of AISI 301

The phase amounts were determined using the direct comparison method [5]. Three phases were found, but only austenite and ά-martensite are considered throughout this study. The ε-martensite only occurred in amounts below 3% and this phase is considered of minor importance for the prediction of mechanical properties.

2.2 Constitutive model

The material model used is an extended Olson-Cohen model to incorporate strain-rate, and stress state dependence. No temperature measurements were performed, but this variable is needed since one of the main effects from high strain rates are adiabatic heating of the sample. The ά-martensite formation can be calculated by the following expressions [6, 7]:

$$\dot{X}_M = (1 - X_M)(A\dot{\bar{\varepsilon}}_\gamma + B\dot{K}_\sigma) \tag{1}$$

With,

$$A = \alpha p \eta n (X_{sb})^{n-1}(1 - X_{sb}) \tag{2}$$

η and n are geometrical constants, while

$$B = \eta X_{sb}^n \frac{dp}{dg} H\left(\frac{dp}{dg}\right) \tag{3}$$

$$K_\sigma = \frac{\sigma_1 + \sigma_2 + \sigma_3}{3\bar{\sigma}} = \frac{1}{3} \tag{4}$$

$$\alpha = (\alpha_1 T^2 + \alpha_2 T + \alpha_3 - \alpha_4 K_\sigma)(\frac{\dot{\bar{\varepsilon}}_\gamma}{\dot{\bar{\varepsilon}}_{ref}})^M \tag{5}$$

$$p(g) = \frac{1}{\sqrt{2\pi}\sigma_g} \int_{-\infty}^{g} \exp\left\{-\frac{(g' - g_0)^2}{2\sigma_g^2}\right\} dg' \tag{6}$$

$$g = -T + g_1 K_\sigma \tag{7}$$

Thus the ά-martensite evolution with true strain can be computed and if accurate predictions are made a simple stress-strain algorithm can be used to describe the mechanical properties [7].

3. RESULTS AND DISCUSSION

The ά-martensite fraction as a function of cold rolling reduction is plotted in Fig. 4. It is seen that the ά-martensite develops in a sigmoidal transformation behavior for cold rolling. It is also observed that the amount of ά-martensite is quite different when comparing the surface and the interior. This is expected due to the different stress states in the centre of the sheet (compression) and at the surface (shear). For the steel sheet suffering 42% cold rolling reduction the ά-martensite fraction at the surface was 29%, but only 20% in the centre. It is therefore a clear benefit to use a bulk method, such as high-energy x-ray diffraction, to determine the phase amounts. However, these measurements showed a phase fraction very close to the phase fraction in the centre of the sheet.

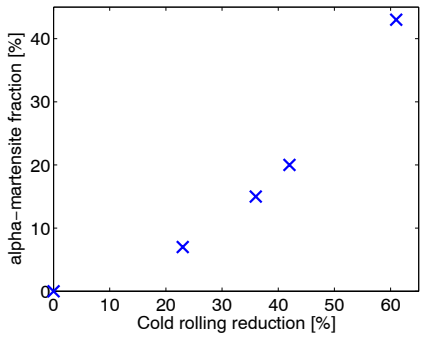

Fig. 4: ά-martensite as a function of cold rolling reduction

The effect of different strain rates during uniaxial tensile loading is demonstrated in Fig. 5. All transformation curves show a sigmoidal transformation behavior and the general trend is well predicted by the used model. A slight increase of the strain rate from 10^{-4} s^{-1} to 10^{-3} s^{-1} increases the amount of ά-martensite and it also changes the transformation kinetics. This behavior is explained in the literature as the competing mechanisms between conventional slip and shear-band formation which supposedly are preferential nucleation sites for ά-martensite [3]. Since the material model is based on this assumption it is also successful in predicting this increase of ά-martensite. A further increase of strain rate

to 10^{-2} s^{-1} is sufficient to alter the amount of transformation drastically. This moderate enhancement of the strain rate generates adiabatic heating of the sample which lowers the amount of martensite, also predicted by the model.

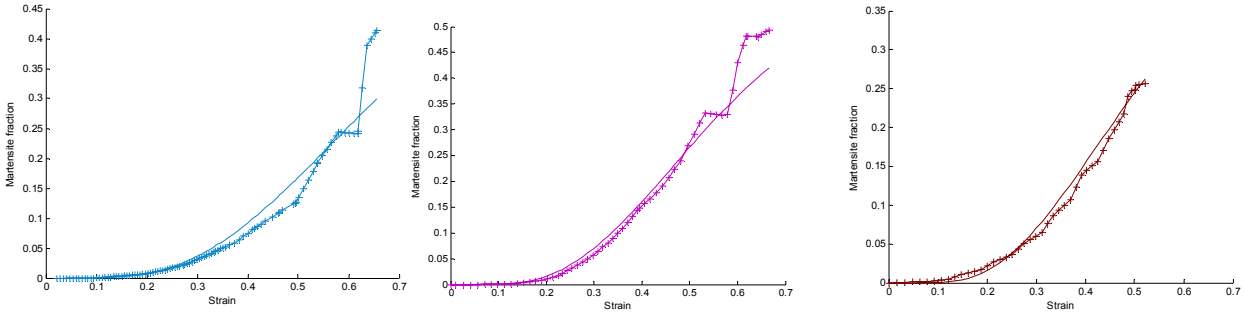

Fig. 5: Strain verses ά-martensite fraction a) 10^{-4} s^{-1} b) 10^{-3} s^{-1} c) 10^{-2} s^{-1}

4. SUMMARY

High-energy x-ray diffraction and material modeling was used to investigate the strain-induced ά-martensite transformation in AISI 301. The effect on strain-induced martensite transformation by two different deformation modes (cold rolling and uniaxial tensile loading) was studied. In addition, three different strain rates for the uniaxial tensile loading were evaluated. A small change of strain rate from 10^{-4} s^{-1} to 10^{-3} s^{-1} increased the amount of martensite transformation and changed the transformation kinetics. This increase of martensite can possibly be explained by the preferred formation of shear-bands instead of conventional slip.

The strain-induced martensite transformation kinetics for all the tested strain rates during uniaxial tensile loading was well predicted by the used material model.

ACKNOWLEDGMENTS

AMASE student Tao Qian is acknowledged for the work with modeling and Jon Almer, Ulrich Lienert, Mark Terner, Joel Bernier is thanked for helping with the experiments at the APS. The work was financially supported by the Swedish Research Council and Outokumpu Research Foundation. Use of the Advanced Photon Source was supported by the U. S. Department of Energy, Office of Science, Office of Basic Energy Sciences, under Contract No. DE-AC02-06CH11357.

REFERENCES

[1] VF Zackay, ER Parker, D Fahr, R Busch, Trans ASM 60 (1967) 252.
[2] P Hedström, U Lienert, J Almer, M Odén Scripta Mater 56 (2007) 213.
[3] GB Olson, M Cohen, Met Trans A 6A (1975) 791.
[4] T Angel, JISI (1954) 165.
[5] BD Cullity, in: M Cohen (Ed.) Addison-Wesley Series in Metallurgy and Materials, 3rd edition, Addison-Wesley, Reading, MA, 1967.
[6] Y Tomita, T Iwamoto, Int J Mech Sci 37 (1995) 1295.
[7] LE Lindgren, *Models for forming simulations of metastable austenitic stainless steel,* In 8th International Conference on Numerical in Industrial Forming Processes NUMIFORM 04, Ohio, USA, 2004.